Mathematical Biosciences and Engineering

MBE, 20 (5): 8400–8427.
DOI: 10.3934/mbe.2023368
Received: 25 September 2022
Revised: 01 January 2023
Accepted: 02 January 2023
Published: 02 March 2023

http://www.aimspress.com/journal/MBE

Research article

An efficient, lightweight MobileNetV2-based fine-tuned model for COVID-19 detection using chest X-ray images

Shubashini Velu*

Department of Management Information System, College of Business, Prince Mohammad Bin Fahd University, 617, Al Jawharah, Khobar, Dhahran, Saudi Arabia

* **Correspondence:** Email: svelu@pmu.edu.sa; Tel: +96656809387.

Abstract: In recent years, deep learning's identification of cancer, lung disease and heart disease, among others, has contributed to its rising popularity. Deep learning has also contributed to the examination of COVID-19, which is a subject that is currently the focus of considerable scientific debate. COVID-19 detection based on chest X-ray (CXR) images primarily depends on convolutional neural network transfer learning techniques. Moreover, the majority of these methods are evaluated by using CXR data from a single source, which makes them prohibitively expensive. On a variety of datasets, current methods for COVID-19 detection may not perform as well. Moreover, most current approaches focus on COVID-19 detection. This study introduces a rapid and lightweight MobileNetV2-based model for accurate recognition of COVID-19 based on CXR images; this is done by using machine vision algorithms that focused largely on robust and potent feature-learning capabilities. The proposed model is assessed by using a dataset obtained from various sources. In addition to COVID-19, the dataset includes bacterial and viral pneumonia. This model is capable of identifying COVID-19, as well as other lung disorders, including bacterial and viral pneumonia, among others. Experiments with each model were thoroughly analyzed. According to the findings of this investigation, MobileNetv2, with its 92% and 93% training validity and 88% precision, was the most applicable and reliable model for this diagnosis. As a result, one may infer that this study has practical value in terms of giving a reliable reference to the radiologist and theoretical significance in terms of establishing strategies for developing robust features with great presentation ability.

Keywords: chest X-ray; deep learning; machine learning; MobileNetv2; SARS-COV-2; transfer learning

1. Introduction, bibliography review and objectives

1.1. Introduction

As a result of the new coronavirus (COVID-19) sickness, millions have died and more have been infected. The World Health Organization declared a pandemic owing to the severity of the outbreak's effects. In December of 2019, it emerged in Wuhan, China, and it has since expanded to 213 countries and territories throughout the globe. As of May 22, 2021 [1], there were 166,632,933 diagnoses and 3,460,809 fatalities in the world (traced at http://covid19.who.int).

In these exceptional times, science and technology have played a crucial role in the execution of policies [2]. Hospitals rely on robots to provide food and medication to COVID-19 patients, and researchers are working around the clock to create novel treatments [3]. Significant contributions have been made by computer scientists who have employed X-ray and computed tomography (CT) images to conduct research on automated coronavirus detection [4]. Significant contributions to the progress of human existence have been made by advances in machine learning; therefore, it is thought that adequate machine learning research plans will fully use machine learning capabilities and aid in the defeat of this horrible illness.

COVID-19 is a contagious disease, and the purpose of this study is to prevent its misinterpretation and misdiagnosis. The coronavirus has severely affected a great number of people from all over the world. Therefore, this condition must be treated as quickly as possible by incorporating technological advancements and machine learning models that will aid practitioners in accurately identifying the disease and preventing misdiagnoses that could result in more damage. Consequently, it is vital to conduct studies in this field because this is a relatively new subject, so there is much potential for further study and investigation. If researchers use machine learning and artificial intelligence to combine additional features from related studies, a more accurate and reliable model can be constructed.

COVID-19-caused pneumonia shares similar symptoms with other types of pneumonia [5]. Consequently, this study also classifies bacterial and viral pneumonia; 450 million individuals are affected by pneumonia annually around the world. In 2016, it ranked as the fourth-largest cause of death in the United States of America. As a result, the most difficult approach is to construct strong and robust features with abundant data and significant discrimination from the relatively few COVID-19 samples. Therefore, the classification of bacterial and viral pneumonia within COVID-19 is an essential area of research.

1.2. Bibliography review

Three years ago highly contagious virus, COVID-19, stunned the world, and countries were placed on lockdown to prevent its spread. Extensive effort has been expended in an effort to detect this disease by using x-rays. The Radiological Society of North America indicated that X-rays can identify COVID-19 because they revealed white patches in the lower corners of the lungs. Radiologists use the term ground glass opacity to characterize the partial filling of the air spaces [11]. Studies have utilized X-rays, CT scans and ultrasound images since then. The difficulty was exacerbated by the fact that computer scientists were investigating numerous machine learning algorithms to many health-related ambiguities.

This area of study is becoming increasingly common. However, each inquiry utilizes a unique sort of dataset. There are numerous imaging modalities accessible in the medical field. This includes,

among others, X-ray imaging, fluoroscopy, magnetic resonance imaging, ultrasound imaging, and CT. Coronavirus diagnostic tests include X-rays, CT scans and ultrasounds. On the basis of the employed dataset, the literature has been evaluated.

Previous research has employed support vector machines (SVMs) as an alternative to convolutional neural networks (CNNs), which require large datasets for training and validation [1]. However, in this study, we employed a large dataset because the model needs to be trained in order to implement clinical context. Due to the restricted range of data, the SVM was able to realize 98% accuracy. As a result of the smaller dataset used to train the model, the model precision may not be characterized as extremely accurate, even though it achieved 98%. Since the extensive data utilized to train the model deal with biological and health contexts, the CNN model may have shown poorer precision in this study. These drawbacks are especially relevant in the current context of a pandemic. Notably, in today's environment, a speedy response is required in places where healthcare systems are overburdened.

In a study conducted by Narin et al. [12], the CNN models ResNet50, InceptionV3 and Inception-ResNetV2 were utilized. They recommended employing chest X-ray radiography to identify people infected with the coronavirus. Their data originated from the open GitHub repository of chest X-rays of COVID-19 patients maintained by Dr. Joseph Cohen. The other half of the dataset, consisting of conventional chest X-rays, was obtained from the Kaggle repository. They had a total of 100 photographs, 50 of which were from COVID-19-positive patients, and the remaining 50 from healthy persons. To compensate for a shortage of data, they utilized transfer learning techniques. To aid training and testing, their dataset was randomly split 80:20 to facilitate training and testing. For the sake of precision, a five-step validation process was done. One of their models, ResNet50, was demonstrated to have an accuracy rate of 98%. Inception-ResNetV2 was utilized to get an accuracy of 87%.

In another study, Panwar et al. [13] utilized deep learning to aid in the detection of coronaviruses. To train the CNN model, they used photographs of healthy and coronavirus-infected lungs. X-ray images served as inputs for the model. They utilized the same data as in the preceding study. The study included 147 COVID-19-positive people and 142 healthy subjects. Previously trained VGG16 models were used to extract features. Due to a shortage of data, transfer learning was implemented. They achieved an accuracy of 88.10%.

Sethy et al. [14] created a novel classification model for healthy people, pneumonia patients and COVID-19 patients. They obtained the data necessary for their investigation from a variety of sources. Their data came from three sources: GitHub, Kaggle and an earlier study by Kermany et al.[28]. Twenty-five infected and 25 non-infected chest X-rays were included in the researchers' data collection. Feature extraction was performed by using VGG16, VGG19, ResNet18, ResNet50, ResNet101, GoogleNet, InceptionV3, InceptionResNetV2, DenseNet201, ShuffleNet, XceptionNet, MobileNetV2 and AlexNet. An SVM was used to categorize the extracted features from the network's SVM, and by utilizing ResNet50 features, it achieved 95.33% accuracy. An F1-score of 98.66% and a sensitivity of 95.33% were also attained by the model used in this study. It also had the lowest rate of false positives, at 2.33%, which is a considerable advantage.

Alqudah et al. [15] developed a model that uses X-ray images to differentiate between healthy individuals, pneumonia patients and coronavirus patients. Using a CNN and a softmax classifier, they evaluate the data. The CNN was also used to extract features, which are then sent to SVM, random forest (RF) and k-nearest neighbor (KNN) classifiers. From Kaggle and GitHub, they added data to the photographs. In total, 600 photographs were included in the collection. The CNN models utilized

AOCTNet, MobileNet and ShuffleNet pre-trained models. Transfer learning was utilized to train the models due to a dearth of training data. To increase the accuracy of the data, a 10-k-fold cross-validation was employed. MobileNet was found to be the most accurate of the three models, with a 99.46% accuracy.

Apostolopoulos and Mpesiana [16] and Xu et al. [17] investigated a technique for identifying COVID-19 in X-ray images. They utilized numerous CNN models. They applied the models to two distinct datasets and compared the results in their studies. In the first dataset, both COVID-19 patients and healthy individuals were included. Due to the lack of large datasets for CNN model training, transfer learning was implemented. The CNN models utilized in these studies include VGG19, MobileNetV4, Inception, Xception and InceptionResNetv2. All of them are triggered by using a rectified linear unit (ReLU) with the Adam optimizer. They evaluated two forms of precision: first, the ability to classify patients into three subgroups: normal, pneumonia and COVID-19. Positive or negative COVID-19 scores were used to determine the second accuracy. For Datasets 1 and 2, they concluded that the most accurate models were VGG19 and MobileNetv2, with MobileNetv2 being the most accurate.

Hussein et al. created a COVID-19 detection technique based on deep learning [18]. A 22-layer CNN model was utilized. The model consisted of nine convolutional layers and nine max pooling layers. Their objective was to construct models capable of detecting between two and four classes. The two subcategories of the two-class classification were normal and COVID-19. There were three classification options: normal, COVID-19 and bacterial pneumonia. Normal, bacterial and viral pneumonia were separated into three categories: COVID-19, bacterial and viral pneumonia. Sigmoid and leaky ReLU functions were used to activate the layers. The dataset comprised a compilation of photographs from various sources. There were around 7390 photographs in their collection. Two courses were properly classified by 99.1% of the models, three classes by 94.3% and four classes by 91.2%.

The objective of Xu et al. [17] was the early diagnosis of pneumonia caused by the influenza-A virus, healthy persons and COVID-19 patients. They generated their dataset by using CT scans from multiple hospitals in Zhejiang province, China. There were about 600 CT scans accessible. Here, they utilized two distinct models. The data were initially preprocessed in order to identify useful lung regions. Following this, a 3D CNN model was utilized to segment the candidate picture cubes. A computerized image classification algorithm eventually classified the photos into three groups: influenza-A viral pneumonia, healthy and COVID-19 patient. Using ResNet, feature extraction was carried out. A network model was then augmented with an additional location-attention mechanism to perform the categorization. Their investigation revealed that the location-attention mechanism model was the most accurate, with an astonishing 86.7% accuracy rate.

In addition, Wang et al. used 453 CT scan images and deep learning techniques to detect COVID-19 [19]. In hospitals, patients with COVID-19 and typical viral pneumonia were surveyed. A radiologist was employed to randomly select areas of interest (ROIs), followed by the training of a CNN model to extract characteristics. Finally, the categorization models provided predictions by using a network that is fully connected. Utilizing an Inception network facilitated the flow of knowledge. Adaboost and a decision tree were implemented to enhance performance. In training, they attained an accuracy rate of 82.9%, but, in testing, it was 73.1%.

Li et al. developed a deep learning strategy to distinguish patients with COVID-19, community-acquired pneumonia (CAP) and healthy persons by using over 4500 CT scan images [20]. The hospitals

furnished them with the necessary information. Using a U-net segmentation technique, the 3D CT scan images were preprocessed to identify the lung ROIs. Using a ResNet50-based network, they created the "COVnet" model, which is capable of generating a three-class likelihood score for patients with COVID-19, CAP and healthy status. The architecture detected COVID-19 with a sensitivity of 90%.

Over 4500 CT scan images were used to classify patients with COVID-19, CAP and healthy persons in another model established by Li et al. [20]. The data were provided by hospitals. The lung regions to be evaluated for the ROI were extracted from the 3D CT scan images by using a U-net-based segmentation technique. COVID-19, CAP and healthy patients could all be assessed by using their model, COVnet, which comprised a ResNet50 network. Additionally, 90% of the time, the architecture was able to detect COVID-19.

Sharma gathered CT scan images of COVID-19, healthy persons and patients with various types of viral pneumonia for their investigation [11]. Before utilizing the dataset, several preprocessing steps, such as image cropping and resizing, were performed to identify vital lung regions. In their analysis, they utilized the ResNet network architecture. Multiple hospitals in China, Italy, Moscow and India contributed their data. They had collected approximately 2200 pieces of information. They spent around 21 hours training the data by utilizing cloud-based training. They were able to get a classification accuracy of 91% with their proposed model. Notably, pneumonia produced by the coronavirus was found to produce a hazy patch that can be exploited by machine learning algorithms to identify the virus in photographs.

Born et al. investigated COVID-19, bacterial pneumonia and healthy patients by using 1100 point-of-care ultrasound imaging (POCUS) with deep CNN models [21]. Using information from Grepmed, Butterfly and the POCUS Atlas, they reached their conclusions. To render POCUS video recordings appropriate for use in deep neural networks, a number of preprocessing and augmentation approaches were applied. Their approach, termed 'POCOVID-net,' utilizes the convolutional component of the VGG-16 model. They achieved an 89% success rate. It was discovered that COVID-19 had a substantial number of false negatives, which must be addressed in future research.

While some studies have used CT imaging and a few have used ultrasound imaging, X-ray imaging has been utilized by the majority of the examined literature. There are some significant differences between the various techniques. CT scans create 3D images, whereas X-rays produce 2D images. The techniques of radiological imaging Unlike X-rays or CT scans, radiography and CT scans are more focused on detecting disease in soft tissues and organs [22]. CT scans and advanced X-rays are similar. When it comes to the diagnosis of throat diseases, X-rays are less expensive than CT scans and offer results that are practically identical to those of CT scans. Since most researchers have used X-ray images as data for their models, the same was done here.

A literature review indicated that deep learning models perform best with image input, and that the vast majority of studies have utilized deep learning models for their research. All of the research utilized a GitHub repository containing X-ray images of normal and COVID-19 patients. In a few investigations, predictions for normal, COVID-19 and pneumonia patients were made. Using Kaggle data, information about pneumonia was obtained. Most researchers have used a pre-trained deep learning model to extract features before passing them to another classifier, such as an SVM, a KNN, an RF or a traditional fully connected layer. As evidenced by the study and the results, several strategies can be utilized as classifiers to examine various outcomes. MobileNet using the KNN classifier has been demonstrated to produce the best results. This research was purposed to establish an imaging-based method for identifying COVID-19 in the bloodstream. Due to the complexity of the issue and

the emergence of new strains of coronavirus, more research must be conducted in this field. Consequently, the ideal model for executing this task has yet to be identified.

Table 1. Summary of all literature.

No.	Research	Main research objectives	Dataset used	Methods used	Validation method	Accuracy
1	Narin et al. (2020)	Automatically predict COVID-19 from X-ray images with the help of CNN models	GitHub repository that was shared by Dr. Joseph Cohen and Kaggle	ResNet50, Inception-ResNetV2 and InceptionV3 used in models applied to an X-ray dataset	ROC curves, confusion matrices using 5-fold cross-validation	RestNet50 98%, InceptionV3 97%, Inception-ResNetV2 87%
2	Panwar et al. (2020)	Automatic screening of COVID-19 from X-ray images using deep learning	GitHub repository shared by Dr. Joseph Cohen and Kaggle	VGG16	Confusion matrix, area under curve (AUC) of ROC and training accuracy plot	88.10%
3	Sethy et al. (2020)	Classify healthy, pneumonia and COVID-19 patient features collected from CNN models and training by applying an SVM to X-ray imaging data	GitHub repository shared by Dr. Joseph Cohen and Kaggle	Deep features collected from VGG16, VGG19, ResNet18, ResNet50, ResNet101, GoogleNet, InceptionV3, InceptionResNetV2, DenseNet201, ShuffleNet, XceptionNet, MobileNetV2 and AlexNet and fed into an SVM	Accuracy, sensitivity, FPR and F1-score were used to evaluate the results	ResNet50+SVM 98.66% as the highest accuracy
4	Alqudah et al. (2020)	Detection of COVID-19 by utilizing lightweight X-ray images and CNN models	GitHub repository shared by Dr. Joseph Cohen and Kaggle	AOCTnet, MobileNet and ShuffleNet used as CNN models; first method: CNN used to classify using softmax; second method: CNN used to extract features and feed them into SVM, KNN and RF	Accuracy, sensitivity and specificity	MobileNet Softmax, MobileNet RF and MobileNet KNN produced highest accuracy of 99.46%
5	Apostolopoulos and Mpesiana, (2020)	Design a 3-class accuracy model for normal, pneumonia and COVID-19 and a binary class model for the presence of COVID-19	GitHub, Internet, by Kermany	Used two different datasets; the CNN models used are VGG19, MobileNetv2, Inception, Exception, Inception ResNetv2	Accuracy, sensitivity and specificity	VGG19 got the highest accuracy: 98.75% for 2-class, and 93.48% for 3-class accuracy.

Continued on next page

No.	Research	Main research objectives	Dataset used	Methods used	Validation method	Accuracy
6	Hussein et al. (2020)	Design a 2-class, 3 class and 4-class classification model including COVID-19, bacterial pneumonia, viral pneumonia and healthy patients	Integrated several datasets together	Used a 22-layer CNN model which consists of nine convolutional layers and nine max pooling layers	Accuracy, precision, recall, sensitivity	99.1% for of 2-class, 94.3% for 3-class and 91.2% for 4-class classification
7	Xu et al. (2019)	Establish early screening model to distinguish pneumonia from influenza-A virus, healthy cases and COVID-19 using deep learning and CT images	Hospitals from Zhejiang province in China	Two CNN models used: ResNet-based model and other models based on location-attention mechanism	Accuracy, precision, recall, F1-score	Model with location-attention mechanism achieved the highest accuracy of 86.7%
8	Wang et al. (2020)	Detect COVID-19 using deep learning methods and CT scans	Collected datasets from hospitals for patients of COVID-19 and typical viral pneumonia	Randomly selected ROIs, trained the model to extract features using Inception-based neural network and transfer learning; then, the classification model was applied for classification	Positive predictive value, negative predictive value, F1-score, accuracy, sensitivity, specificity, AUC, Youden Index	82.90%
9	Li et al. (2020)	Design a deep learning method to enable classification of patients with COVID-19, healthy persons and CAP patients using CT scans	Collected data from hospitals	Preprocessing was done, ROIs were selected; then, a ResNet50-based neural network was used	Sensitivity, AUC of ROC, p-value	Sensitivity of 90% for COVID-19 patients
10	Sharma (2020)	Build a model to classify COVID-19, healthy and other viral pneumonia patients based on CT images	Different hospitals from China, Italy, Moscow and India	Preprocessing involved image cropping and resizing, and they used a ResNet architecture to build the model	Accuracy	91%
11	Born et al. (2020)	Detect COVID-19 using POCUS by applying deep CNN models to three classes: COVID-19, bacterial pneumonia and healthy patients	Grepmed, Butterfly and POCUS Atlas	Preprocessing of lung POCUS videos and augmentation of dataset; VGG16 used	Sensitivity, specificity, precision, F1-score	89%

Note: Table 1 shows the literature that has been reviewed. It is observed that most of the researchers used deep learning models to conduct their study because deep learning models produce the best results with image input. All of the studies used datasets from the GitHub repository of Dr. Joseph Cohen, which is composed of X-ray images of normal and COVID-19 patients.

Deep learning methods in modeling and classification have been successfully applied in a variety of fields, especially the medical imaging domain [6]. This work employed deep learning techniques to

improve the analysis and produce more accurate results [7]. Deep learning architectures have been used to predict a patient's COVID-19 status as positive or negative. The bulk of researchers adopted CNN models, while the optimal model has yet to be established. This study focuses on comparisons, as opposed to determining the best model, as other researchers have done [8, 9]. In this study, CNN models trained from scratch and pre-trained models are compared to determine which is more effective for this purpose. Moreover, this is a crucial study due to the limitations of the two most common approaches for diagnosing COVID-19, i.e., RT-PCR and conventional X-ray. Currently, the most prevalent screening approach is, which is a trustworthy standard, however imaging can be used as a supplement in diagnosing COVID-19. In addition to that, RT-PCR test kits, for instance, are costly and not readily available in a number of nations, especially poor nations [10]. In addition, it takes 4 to 6 hours to get the results, which is a significant period considering the severity of the illness. Moreover, RT-PCR results vary widely from country to country. As false negatives are a significant issue in the medical industry, they may contribute to the transmission of disease. Even a single false negative can have major consequences for a large number of individuals. In contrast, traditional X-ray systems require a radiologist to manually evaluate X-ray images, which is time-consuming. Consequently, it is imperative to create a method of coronavirus identification that is both automatic and capable of delivering highly reliable results. Here is a list of the study's most significant contributions:

- Use a deep CNN model to build a detection model for COVID-19;
- Create a COVID-19 detection model based on a refined ResNet50;
- Use MobileNetV2 to develop a detection model for COVID-19; and
- Investigate and select the optimal deep learning model for detecting the best model.

1.3.Objectives of the study

The main purpose of this study was to further explore deep learning techniques and all of the methods that have been used in the detection of COVID-19 so far. Additionally, the best and most reliable model will be proposed as the ideal framework to be used by medical practitioners and other researchers.

1. Research on techniques and approaches for COVID-19 detection models all around the world.
2. Develop a detection model for COVID-19 by using a deep CNN model.
3. Develop a detection model for COVID-19 by using a fine-tuned ResNet50.
4. Develop a detection model for COVID-19 by using a fine-tuned MobileNetV2.
5. Investigate performances of the proposed deep learning models and identify the best model for detection.

Section 2 includes the methods used in this research. Section 3 presents the details of the data employed for training and testing the proposed machine learning models and reports the results from the design of the experiment. Section 4 discusses and concludes the findings of this research, as well as the limitation and future direction of the research.

2 Methodology

2.1. Summary of methodology

Figure 1 depicts the study's suggested research methodology. A number of steps comprises the proposed methodology. Investigating the issue of greatest interest was the initial phase in undertaking

the study. After completing the research, a number of sources were utilized to collect data. Next, data preparation and study of the optimal model were required. After this step, models were constructed. The best model was then recommended for the categorization assignment after a comparison of both models.

All of the photographs were offered in various sizes. To guarantee uniformity across the models, each photo was scaled to the same end dimensions. The new resolution was 224×224×3. There was more data enhancement, including horizontal/vertical shifting, flipping and rotation. This also assists the models in learning about all conceivable data changes. This was done so that the images would be more diversified and the model would be less susceptible to overfitting. In addition, each pixel in the training images was converted from the range [0, 255] to the range [0, 1]. The performance of the model was not negatively impacted by a single outlier pixel. The training images underwent shear and zoom modifications of 0.2, as well as a horizontal flip. The settings were such that, if you do not need to contribute new data, you can utilize data augmentation to increase the diversity of your existing data. From the data, a training set and a validation set were generated. Due to the fact that the CNN does not require a great deal of image processing, minimal cropping and scaling were required.

2.2. CNN

CNNs are one type of artificial neural network (ANN). ANNs and other supervised learning algorithms are based on the concept of biological neural networks [23]. Two researchers found these concepts while attempting to emulate brain functions. Akin to the human brain, an ANN may perform multiple jobs. In an ANN, which is a single unit, a neuron is a mathematical function that assembles and categorizes input based on a specific design. ANNs, like regression and curve fitting, are statistical methods. Neurons are the primary component of the brain, and they are structured in various layers with numerous interconnections. The input layer, hidden layer, and output layer are the three most fundamental elements. When multiple layers are placed on top of one another, this is regarded as deep learning.

CNNs comprise layers such as a convolutional layer, nonlinearity layer, pooling layer and fully connected layer [24], in addition to the fundamental ANN layers. Figure 2 depicts a basic CNN model concept. CNN functions resemble those of the visual cortex significantly. First, the computer converts the image into a matrix based on the image type and size. One pixel is utilized for grayscale images, while three pixels are required for RGB images. The purpose of a convolutional layer is to reduce the size of the matrix and give a simpler format, which facilitates processing and prevents the loss of essential properties. A feature detector, i.e., a small filter employed in the convolutional layer, processes the input image matrix before performing computations. This is done so that a feature map may be generated from the bigger input matrix. This method facilitates the elimination of a large number of irrelevant attributes. The most essential characteristics are reserved for the subsequent layer. After the convolutional layer comes the nonlinearity layer. The nonlinearity layer includes an activation function to generate nonlinearity. In order to accurately anticipate the class labels, the network must be nonlinear. Sigmoid, tanh, ReLU and softmax activation functions are applied, among others. Sigmoid functions are frequently applied for binary classifications. The subsequent layer is a layer that executes the actual pooling operation. This is done to remove less important features from the feature map and retain only the most important ones. This reduces the feature map's file size, making it easier to process the data. Max pooling, sum pooling, average pooling, etc., can all be utilized for pooling [6] The result of this layer is a combined feature map. The feature map is flattened into a long vector for usage by the ANN as the final phase. In the completely linked layer, a number of nodes

resemble a number of target classes. For training purposes, a stated learning rate is also provided. Low learning rates are utilized to accelerate the training process, whereas higher learning rates increase generalization [5].

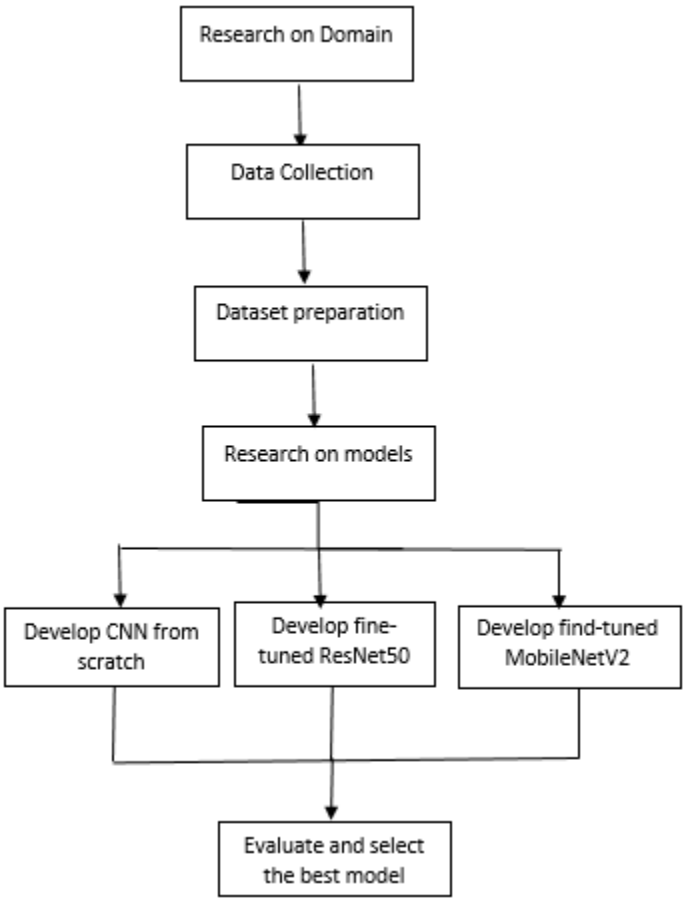

Figure 1. Flowchart of proposed methodology.

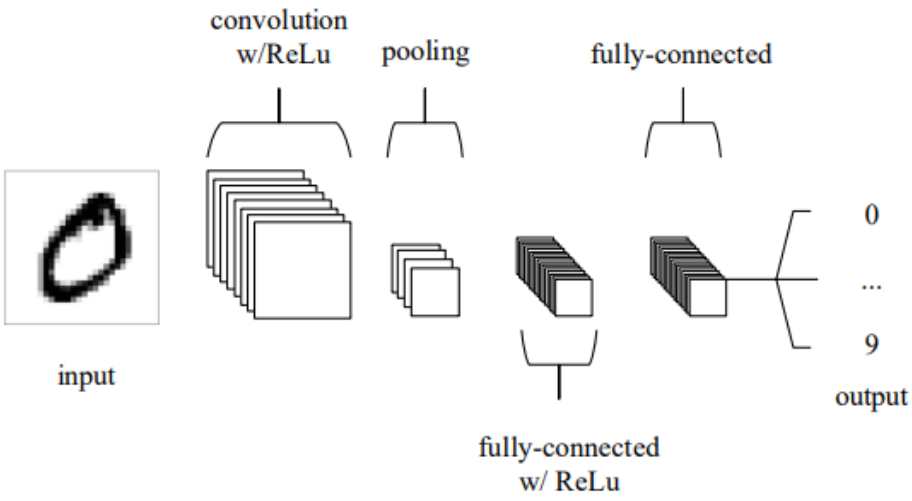

Figure 2. Simple CNN from O'Shea and Nash [3].

2.3. Transfer learning

The literature concerning COVID-19 employs transfer learning. It has become a common technique in computer vision due to its rapidity and accuracy in constructing models. It is typical to require a large quantity of data to train a deep learning model (i.e., data that are not always readily available). The labeling of data by specialists is extremely time- and cost-intensive, particularly for medical information. Consequently, transfer learning enables the training of data with a smaller dataset, and at a cheaper cost in these situations. These models can then be transferred to a new model that will be trained by using a smaller dataset.

This overcomes the issue of having to start from scratch while learning a new skill. In this research, pre-trained models trained on similar domains were utilized. This allowed for selection from pre-trained deep learning models such as ResNet, ResNetV2, VGG16, VGG19, InceptionV3 and MobileNet. This study utilized ResNet50. It is identical to a CNN, except that it has additional features. The ImageNet database was used to train the 50-layer neural network ResNet50. The majority of ResNet models are highly accurate, showing that ResNet models are among the best models to use in a particular circumstance.

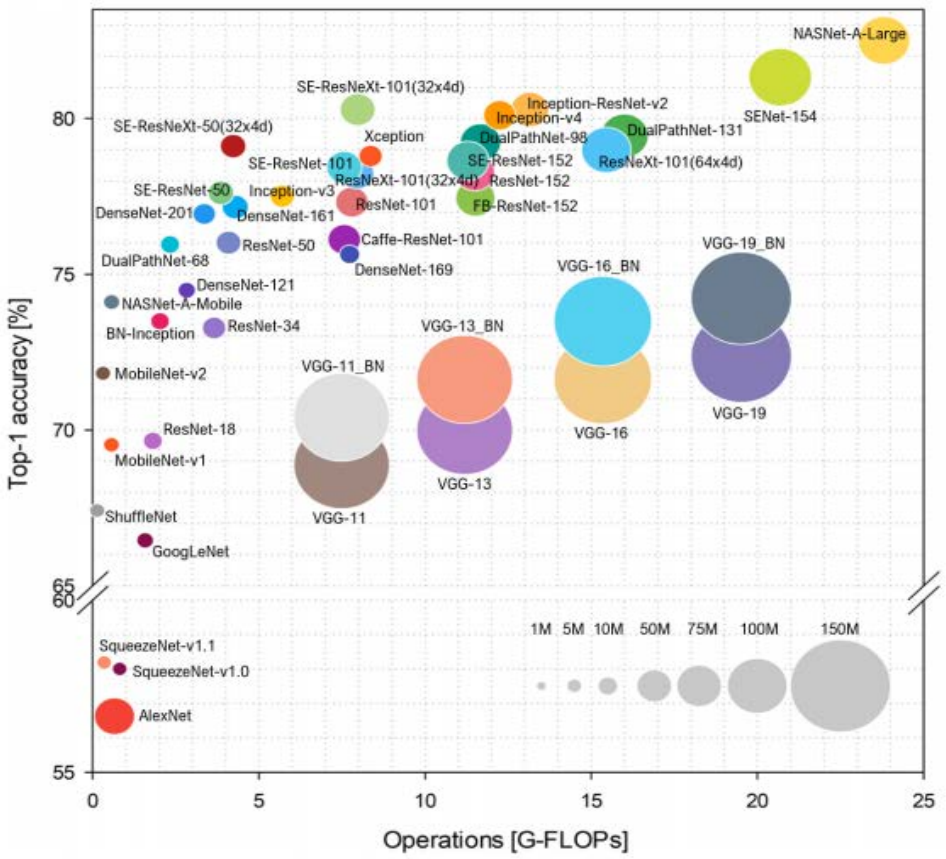

Figure 3. Image classification accuracy vs. operations.

First, the pre-trained model is employed as a feature extractor; second, the pre-trained model is fine-tuned with a feature extraction algorithm. Using pre-trained models as feature extractors was made possible by freezing the convolutional blocks and replacing the fully connected layer. The convolutional layers are frozen between epochs to prevent weight updates. The bottleneck features are depicted on the activation feature map formed by the final block of convolutional layers in the pipeline.

To learn the new task, these elements are added to the final, fully connected layer. The pre-trained model's fully connected layer is subsequently deleted and replaced with a new fully connected layer. Alternatives to the final fully connected layer include logistic regression, an SVM and other lightweight linear models.

The convolutional layers of the pre-trained model are frozen, followed by the fine-tuning of the remaining layers. This permits the complete model to be trained while final parameter adjustments are done. The first and second layers of a network collect generic data, but the third and fourth levels collect data specific to a particular dataset [25]. Inception ResnetV2, along with VGG-19, MobileNet and Resnet50, is a notable model. Figure 3 shows a graph containing all of the pre-trained models. It can be seen that most of the ResNet models are on the side with high accuracy, showing that ResNet models are some of the best models to be used.

2.4. Data exploration

Figure 4 shows the averages of pixels of every class. A matrix was formed from the image pixels. After creating the matrix, the average pixels were calculated. Grey color maps were used to create the average images. These images show that, on average, the COVID-19 X-ray images had the highest obstruction and blurriness around the chest area, and that the least obstruction was present in the normal X-ray images. Meanwhile, average bacterial and viral images were also observed to have some obstruction, although it was less than the obstruction of the COVID-19 images.

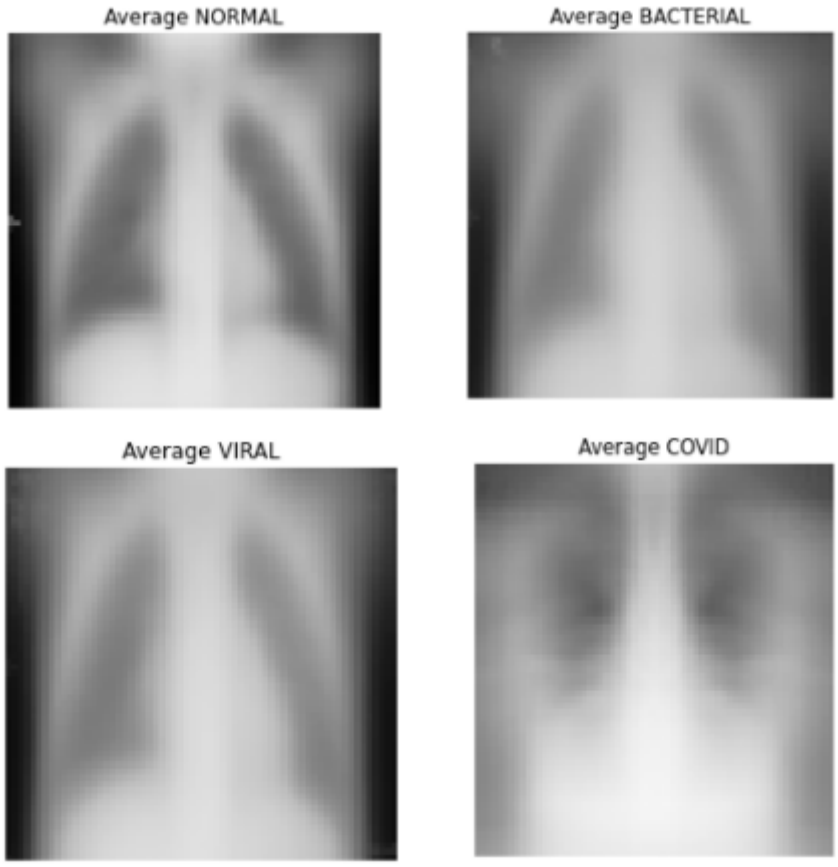

Figure 4. Averages of pixels of every class.

2.5. Eigen images

Eigen images were produced as a part of data exploration. Eigen images are ordinarily the eigenvector of principal component analysis of the image matrix. These images are useful when there is a requirement of dimensionality reduction. These images create visualizations which explain 70% of the variability in each respective class. Figure 5 shows the eigen images of the normal patients. It can be observed that the edges of ribs and other organs were defined clearly in the eigen images of normal patients, as opposed to the other classes. It can also be observed in Figure 8 that the eigen images of COVID-19 had the blurriest and most undefined edges. Additionally, the number of principal components was largest for normal patients, while it was the smallest for COVID-19 patients. The principal components were sets of features formed from initial features to reduce the number of total features.

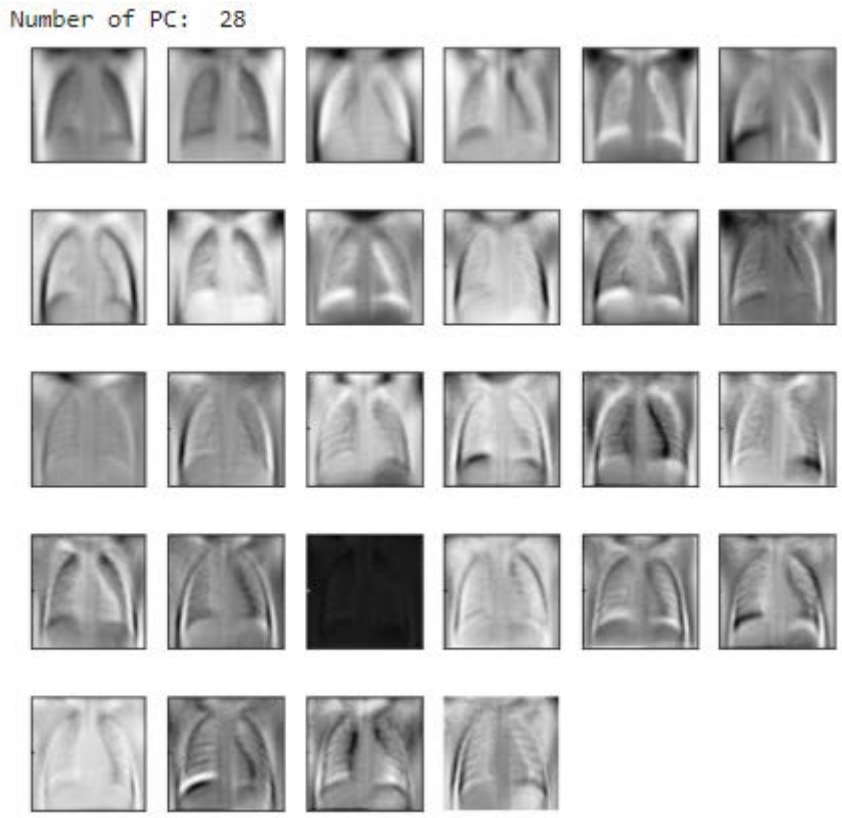

Figure 5. Eigen images of normal X-ray images.

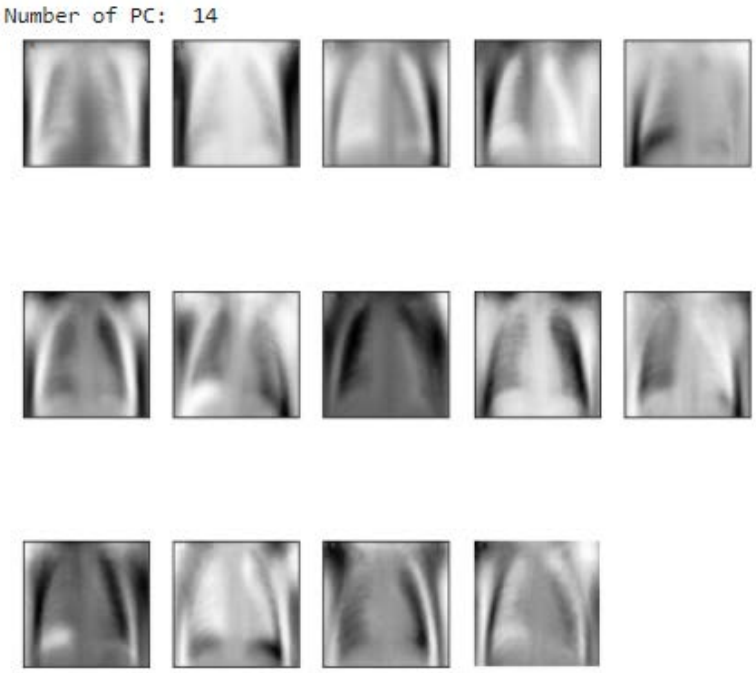

Figure 6. Eigen images of bacterial X-ray images.

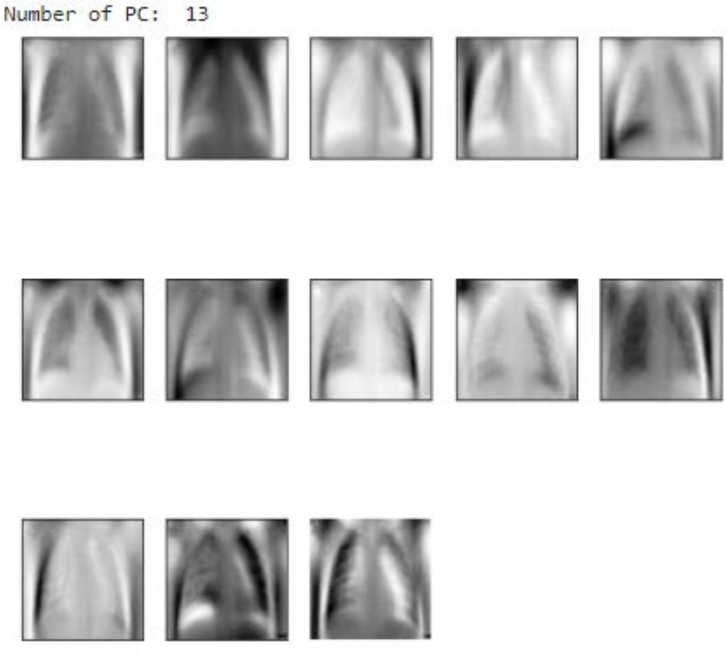

Figure 7. Eigen images of viral X-ray images.

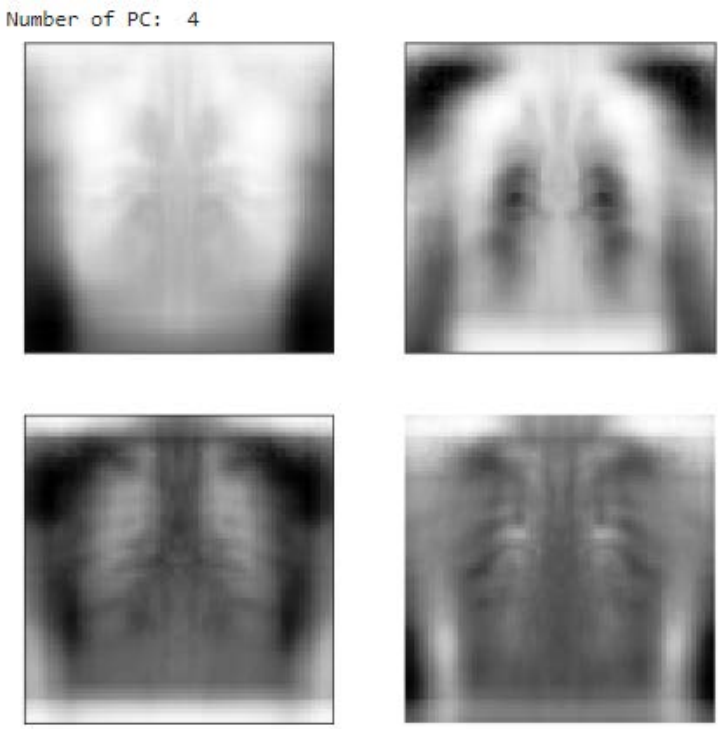

Figure 8. Eigen images of COVID-19 X-ray images.

2.6. Development of Deep CNN model (Model 1)

In this initial model, a CNN was trained from scratch. There are 13 layers in this model. There are initially two convolutional layers, each containing 16 and 32 convolutional units. The standard kernels consisted of three bytes. Since the images were scaled down to 224×224 and were RGB, the input form was 224×224×3. Immediately following two convolutional layers is a max pooling layer with a 2×2 pool size. Following the two preceding convolutional layers is a further convolutional layer and a max pooling layer. In each of these two layers, 64 and 128 convolutional units are present. Following that, there are two further convolutional layers with 256 and 512 units, as well as a final layer containing all of the data. All convolutional layers are activated by a ReLU activation function. In the final process, a flattening layer is applied. At the conclusion of the network are two extremely dense layers. After the initial 512-unit dense layer, a 0.6-rate dropout layer is introduced. In the final dense layer, there are four categories to identify; therefore, there are four units in this layer. This layer uses the softmax classifier to activate it. To optimize the model, the Adam optimizer is employed with a learning rate of 0.0001. Cross-categorical entropy is applied as the loss function.

Figure 9 depicts the executive summary of the model. The output of the first convolutional layer is a picture with dimensions of 222×222. The output of this layer is 220 by 220 pixels. The number of parameters in the second convolutional layer increased from 448 to 4640. The maximum output of the pooling layer is 110×110. This information is output by the third convolutional layer as a matrix with a resolution of 108×108 and a total of 18496 parameters. In the fourth convolutional layer, over 73856 parameters are created. The precise output of this layer is 53×53. The fifth and sixth convolutional layers produce images with 51×51 and 49×49 pixels, respectively. The sixth convolutional layer contains 1180160 parameters. This model contains 152,570,276 trainable parameters out of a total of 152,570,276.

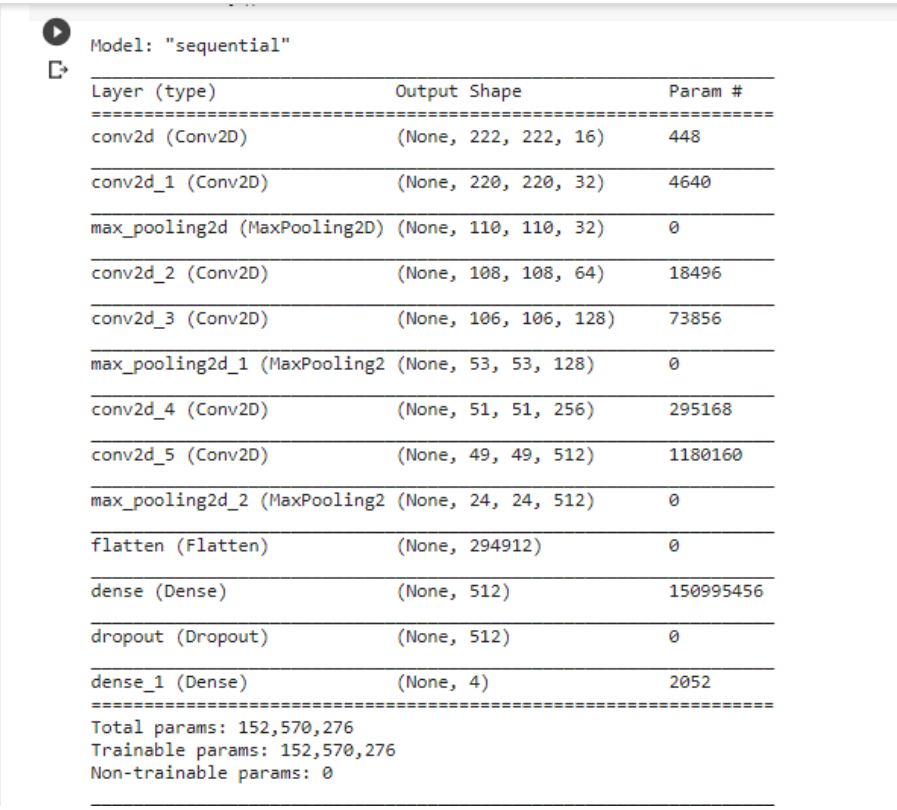

```
Model: "sequential"
_________________________________________________________________
Layer (type)                 Output Shape              Param #
=================================================================
conv2d (Conv2D)              (None, 222, 222, 16)      448
_________________________________________________________________
conv2d_1 (Conv2D)            (None, 220, 220, 32)      4640
_________________________________________________________________
max_pooling2d (MaxPooling2D) (None, 110, 110, 32)      0
_________________________________________________________________
conv2d_2 (Conv2D)            (None, 108, 108, 64)      18496
_________________________________________________________________
conv2d_3 (Conv2D)            (None, 106, 106, 128)     73856
_________________________________________________________________
max_pooling2d_1 (MaxPooling2 (None, 53, 53, 128)       0
_________________________________________________________________
conv2d_4 (Conv2D)            (None, 51, 51, 256)       295168
_________________________________________________________________
conv2d_5 (Conv2D)            (None, 49, 49, 512)       1180160
_________________________________________________________________
max_pooling2d_2 (MaxPooling2 (None, 24, 24, 512)       0
_________________________________________________________________
flatten (Flatten)            (None, 294912)            0
_________________________________________________________________
dense (Dense)                (None, 512)               150995456
_________________________________________________________________
dropout (Dropout)            (None, 512)               0
_________________________________________________________________
dense_1 (Dense)              (None, 4)                 2052
=================================================================
Total params: 152,570,276
Trainable params: 152,570,276
Non-trainable params: 0
_________________________________________________________________
```

Figure 9. Model summary of first model.

2.7. Development of fine-tuned ResNet50 model (Model 2)

The second model utilized a ResNet50 CNN model with fine-tuning. ResNet50 is composed of 50 layers. This model uses several blocks and convolutional layers. The conv4 block1 layer was omitted in order to fine-tune ResNet50. This study's dataset was only utilized to train the initial few layers of the neural network. This refined model eliminates the top fully connected layer of ResNet50 and replaces it with another fully connected layer that is capable of detecting the classes utilized in this study. Once the ResNet50 model has been fine-tuned, the flatten function is applied. The first of two thick layers consists of 512 units with a ReLU activation function. With a 0.66 dropout layer, we proceed to the subsequent layer. The final dense layer, comprised of four units, is activated via softmax activation. The Adam optimizer is used to construct and tune the final model by applying categorical cross-entropy with a learning rate of 0.001.

Figure 10 provides an illustration of the model summary. The output of the ResNet50 layer has 23587712 parameters, as observed; 51380736 features can be extracted from the initial layer of the dense layer. The final data layer produces 2052 parameters. There are a total of 74,970,500 parameters, of which 73,467,396 are trainable and the remainder are non-trainable. During the training process, layers that were kept frozen generate non-trainable parameters.

```
model_2.summary()

Model: "sequential_1"
_________________________________________________________________
Layer (type)                 Output Shape              Param #
=================================================================
resnet50 (Functional)        (None, 7, 7, 2048)        23587712
_________________________________________________________________
flattened (Flatten)          (None, 100352)            0
_________________________________________________________________
dense_1 (Dense)              (None, 512)               51380736
_________________________________________________________________
dropout_1 (Dropout)          (None, 512)               0
_________________________________________________________________
predictions (Dense)          (None, 4)                 2052
=================================================================
Total params: 74,970,500
Trainable params: 73,467,396
Non-trainable params: 1,503,104
```

Figure 10. Model summary for Model 2.

2.8. Development of fine-tuned MobilenetV2 model (Model 3)

The pre-trained MobilenetV2 network is the third model proposed. The network's lower layers are frozen, while the top few blocks are unfrozen for fine-tuning. The fully linked layer of the pre-trained MobilenetV2 model is deleted and replaced with dense layers, allowing it to distinguish between the four categories of diseases. The initial dense layer of MobilenetV2 contains 512 units and is activated by ReLU, whereas the final dense layer contains four units. Using the softmax option, one can enable this additional degree of security. A model can be compiled and optimized by using an Adam optimizer with a learning rate of 0.00001.

```
model_3.summary()

Model: "sequential"
_________________________________________________________________
Layer (type)                 Output Shape              Param #
=================================================================
mobilenetv2_1.00_224 (Functi (None, 7, 7, 1280)        2257984
_________________________________________________________________
flattened (Flatten)          (None, 62720)             0
_________________________________________________________________
dense (Dense)                (None, 512)               32113152
_________________________________________________________________
dropout (Dropout)            (None, 512)               0
_________________________________________________________________
predictions (Dense)          (None, 4)                 2052
=================================================================
Total params: 34,373,188
Trainable params: 33,641,284
Non-trainable params: 731,904
```

Figure 11. Model summary for the third model.

The proposed model is depicted in Figure 11. There are 2257984 parameters in the MobilenetV2 layer, 32113152 parameters in the first dense layer and 2052 parameters in the last dense layer. This model contains 34,373,188 parameters, of which 33,641,281 can be trained and the rest cannot be trained.

3. Results

3.1. Description of dataset

This study's dataset was compiled from two distinct data sources. The first data source [4] comprised X-rays of COVID-19 and other pneumonia types. The data collection also contained front and side X-ray images of each patient's chest, as well as information regarding the patient's condition, survival and hospital location. The data from Kaggle were incorporated into the second dataset. This dataset contained X-ray images of normal, bacterial and viral pneumonia patients [26]. There were 5864 images in all. Train and test picture sets were separated into two distinct sets. In order to correctly evaluate a model, both a training set and a testing set are required. Table 2 displays the quantity of images in each category. In this investigation, the proportion of splitting was 25:75. Seventy-five percent of the images were utilized in the training set, while the remaining 25% were used in the testing set. There were four groups of images: normal, bacterial, COVID-19 and viral. Three instances of image data that were used in the study are depicted in Figures 12, 13, 14 and 15. Figure 12 illustrates an X-ray of the chest of a sufferer of bacterial pneumonia. The chest x-ray of a patient with viral pneumonia is depicted in Figure 13.

Table 2. Splitting of images in the dataset.

	Normal	**COVID-19**	**Bacterial**	**Viral**
Train	1075	1076	1096	1076
Test	269	266	269	269

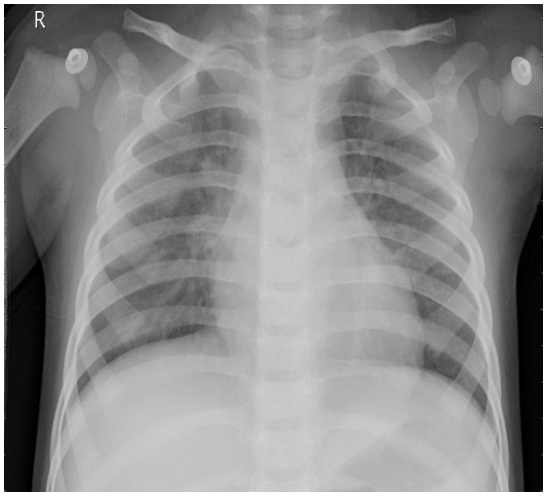

Figure 12. X-ray image of a bacterial pneumonia patient.

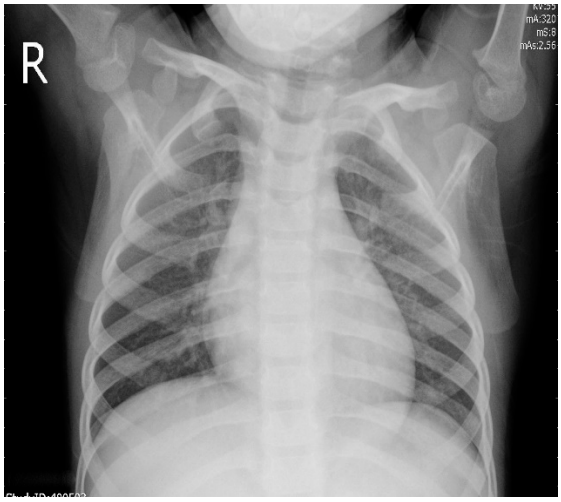

Figure 13. X-ray image of viral pneumonia patient.

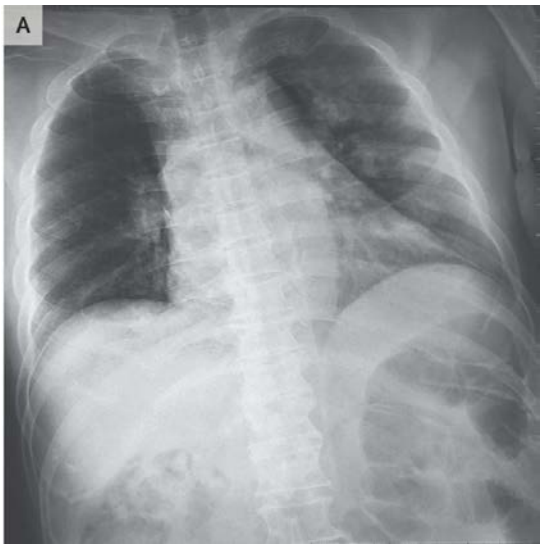

Figure 14. X-ray image of COVID-19 patient.

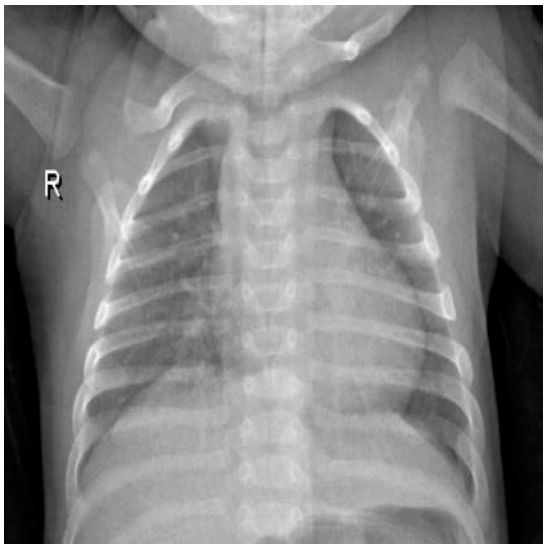

Figure 15. X-ray image of healthy patient.

3.2. Model evaluation

A confusion matrix was constructed to determine whether the forecasts matched the actual findings. The performance of a classifier can be evaluated in this way.

In the confusion matrix, models were evaluated according to five criteria:

1. *Sensitivity = True Positive/ (True Positive + False Negative)*
2. *Specificity = True Negative / (True Negative + False Positive)*
3. *Precision = True Positive/ (True Positive + False Positive)*
4. *Accuracy = (True Negative + True Positive) / (True Negative + True Positive + False Negative + False Positive)*
5. *F1-score = 2 × (Precision × Sensitivity)/(Precision + Sensitivity)*

COVID-19-positive true positives refer to photographs in a particular dataset that have been correctly identified as such. This is the proportion of photographs correctly identified as non-COVID-

19/healthy patients. False positive refers to the proportion of COVID-19-positive images that correspond to healthy X-rays. False negatives refer to the number of photographs containing COVID-19-positive images that are misidentified as healthy images.

The examination was administered by using an accuracy metric. However, judging performance exclusively based on precision increases the likelihood of incorrect results due to the fact that a disparity between classes will not be considered when determining accuracy. This is why the F1-score is utilized in our evaluations. The F1-score exceeds the constraints imposed by class inequality. Precision-recall was also utilized to assess the output quality of the classifier. This indicates that a model with high precision and high recall has a high level of precision and consistency.

Additionally, the performance of the model can be estimated by using these metrics. Considering the severity of this condition, training or testing should also be considered. If the model takes a long time to produce findings, this will be an issue in medicine. If the model is capable of detecting this highly contagious disease, all of these parameters should be considered. The purpose of the evaluation was to assess the models and determine the optimal solution to this problem. This will therefore provide an answer to the issue of whether transfer learning outperforms the deep CNN model.

3.3. Results of Model 1

The model's accuracy was 0.8140, and its loss after 30 epochs was 0.4189. The validation error was 0.2727, while the accuracy was 0.9173. The training accuracy of this model has been demonstrated to be low. The accuracy on both the training and validation data consistently increased throughout the course of all 30 epochs. Additionally, data loss decreased on a regular basis. Regarding the 30 epochs, Figure 16 displays the accuracies and losses of both sets of data.

Figure 17 depicts the categorization report for Model 1. The classification precision and memory for COVID-19 are quite good, whereas those for the other three classes were inferior. Regarding viral pneumonia, the F1-score was 0.65, which was lower than that for any of the other classes, indicating that the model performed poorly. The average precision and recall for the model were 0.84 and 0.83, respectively.

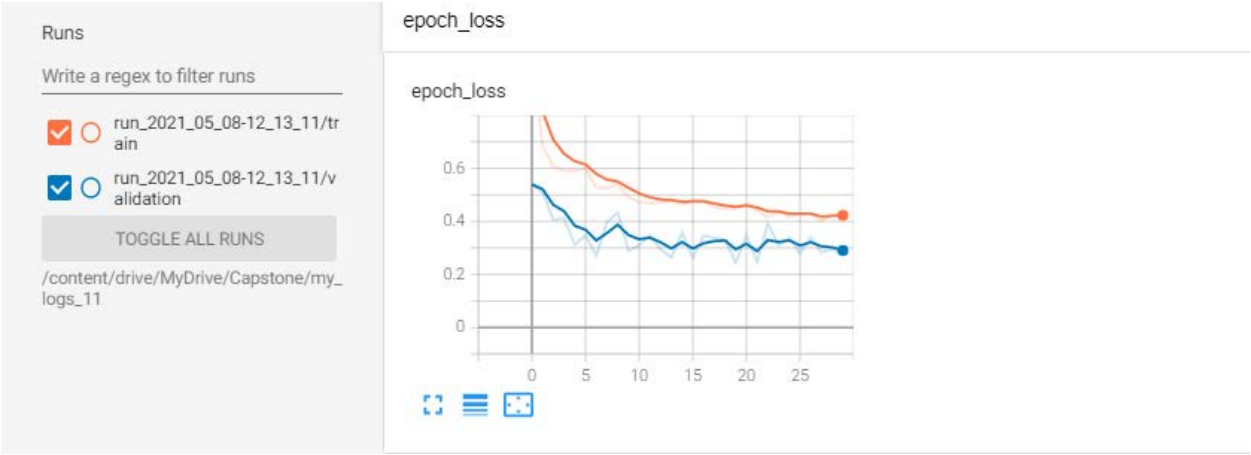

Figure 16. Training and validation accuracy and loss for Model 1.

	precision	recall	f1-score	support
Bacterial	0.69	0.85	0.76	269
Covid	1.00	0.98	0.99	266
Normal	0.87	0.96	0.91	269
Viral	0.80	0.55	0.65	269
accuracy			0.83	1073
macro avg	0.84	0.83	0.83	1073
weighted avg	0.84	0.83	0.83	1073

Figure 17. Classification report for Model 1.

3.4. Results of Model 2

The refined ResNet50 model had a validation loss of 0.5622 and a training loss of 0.4670. The training accuracy was 0.8060, while the validation accuracy was 0.8934. Similarly, this model failed when evaluated against actual data. The precision and losses of both sets of data are depicted in Figure 18. It may be observed that the validation accuracy is extremely inconsistent and fluctuated frequently. The validation losses were similarly enormously huge in the beginning and approach zero by the end.

Figure 19 depicts the categorization reports for Model 2. The COVID-19 classification had the highest F1-score of 0.92. The F1-scores for bacterial and viral pneumonia were 0.53 and 0.51, respectively. When it comes to identifying healthy persons, this model's F1-score was the lowest. The overall average was 0.72, and the recall was 0.56. This demonstrates the level of imprecision and nonsensicality of this paradigm. As a result, the F1-score was 0.49.

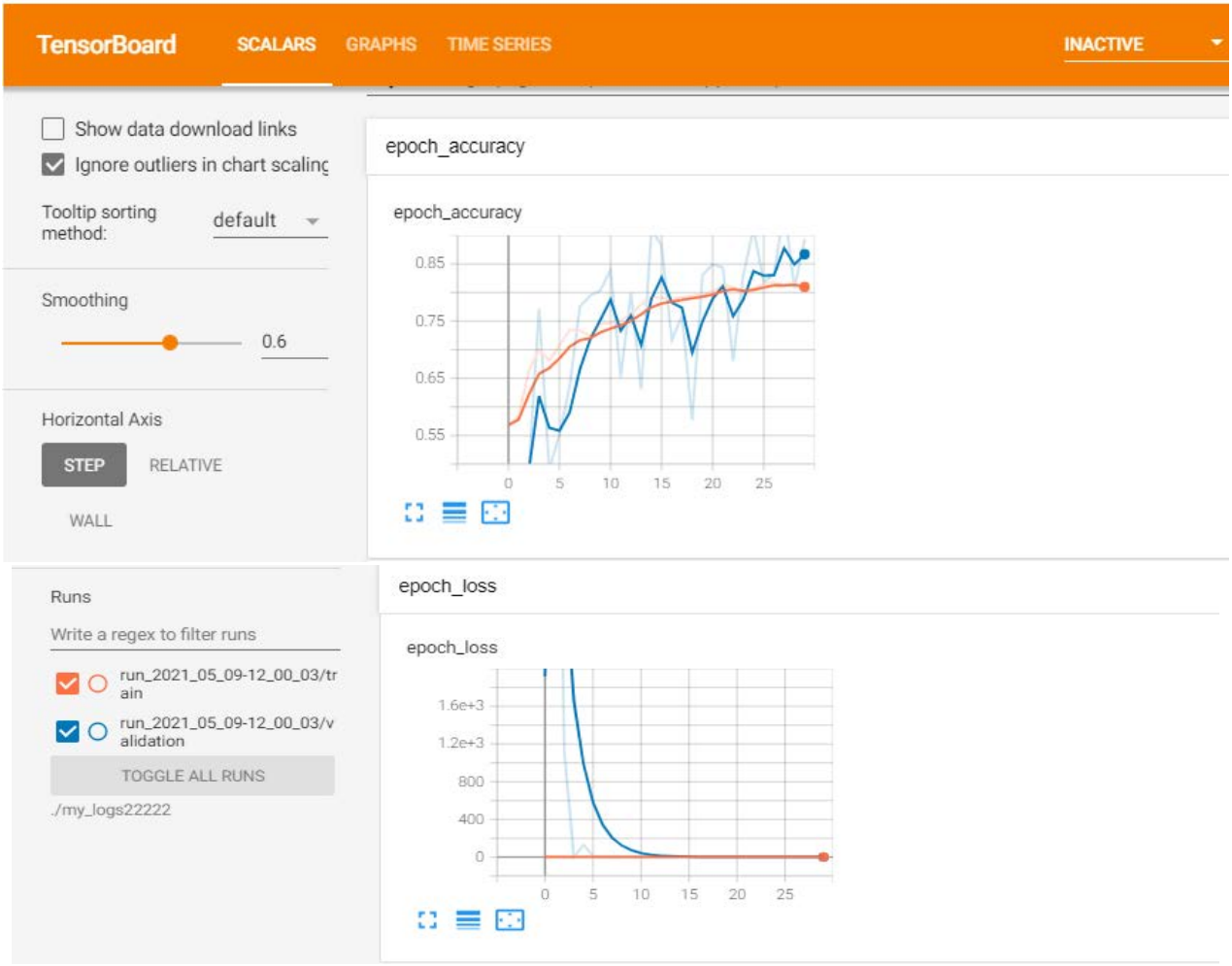

Figure 18. Training and validation accuracy and loss for Model 2.

	precision	recall	f1-score	support
Bacterial	0.39	0.84	0.53	269
Covid	0.86	0.98	0.92	266
Normal	1.00	0.00	0.01	269
Viral	0.61	0.44	0.51	269
accuracy			0.56	1073
macro avg	0.72	0.57	0.49	1073
weighted avg	0.72	0.56	0.49	1073

Figure 19. Classification report for Model 2.

3.5. Results of Model 3

The fine-tuned model of MobileNetV2 produced a training accuracy and loss of 0.9250 and 0.9251, respectively, and a validation accuracy and loss of 0.9375 and 0.1906 for the latter, as shown in Figure 20. Figure 20 depicts this data graphically. The validation accuracy was initially low throughout the first 30 epochs, but it drastically improved near the end of the 30 epochs. The validation and training accuracy scores coincided between the 20th and 30th epochs, confirming their similarity. The training

accuracy improved modestly during the course of 30 epochs.

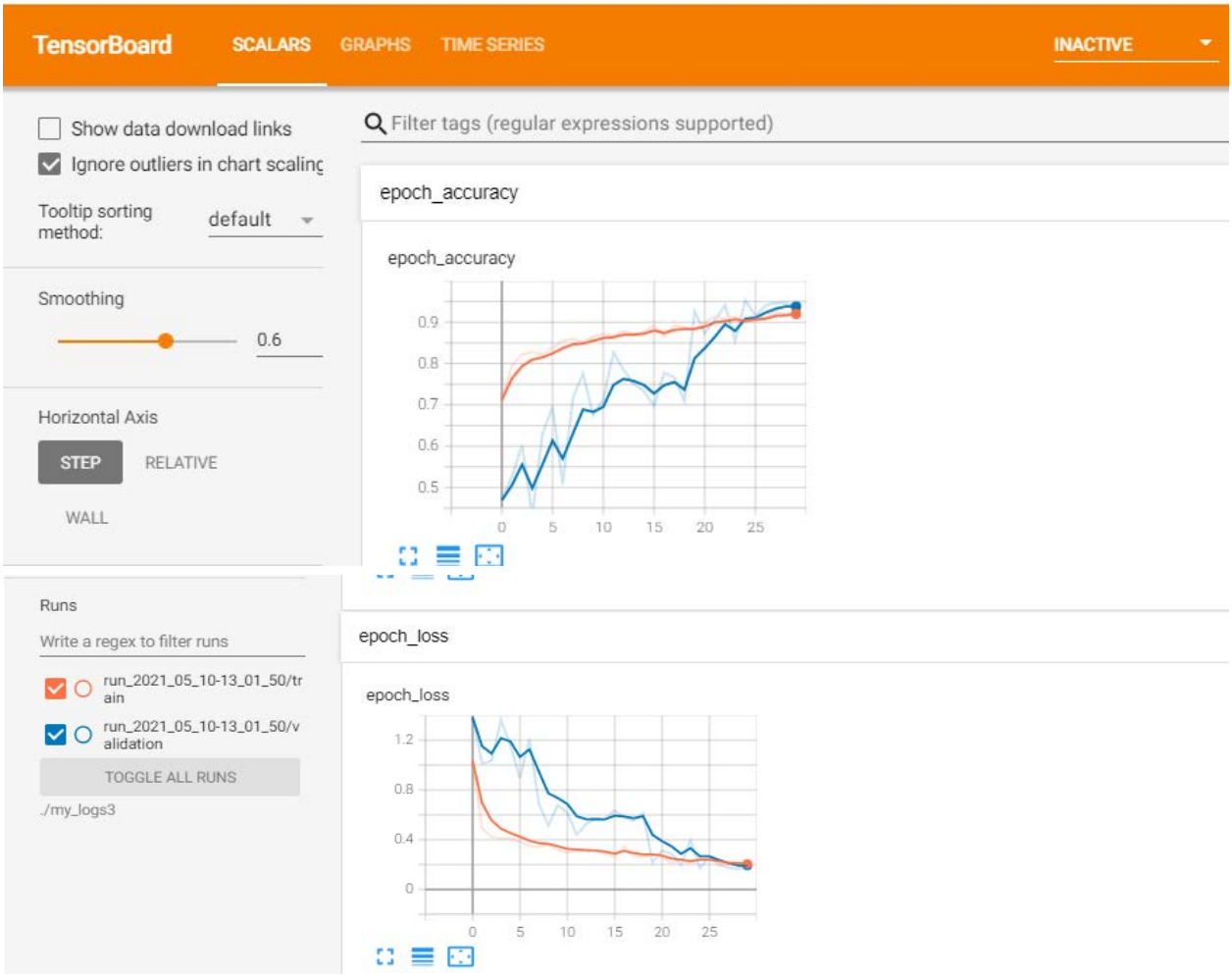

Figure 20. Training and validation accuracy and loss.

Figure 21 depicts the categorization report for the third model. For the entire model, the precision was 0.88 and recall was 0.87. As a result, the F1-score was equally high, at 0.87. The model had the highest precision and recall for the classification of COVID-19 and normal patients. The precision and recall scores for bacterial and viral pneumonia were both below average, showing that the model has difficulty distinguishing between the two forms of pneumonia.

	precision	recall	f1-score	support
Bacterial	0.73	0.88	0.80	269
Covid	1.00	0.99	0.99	266
Normal	0.96	0.96	0.96	269
Viral	0.82	0.66	0.73	269
accuracy			0.87	1073
macro avg	0.88	0.87	0.87	1073
weighted avg	0.88	0.87	0.87	1073

Figure 21. Classification report for Model 3.

3.6. Comparison of results

The three investigated models are summarized in Table 3. Models 1 and 2 were somewhat less precise than Model 3 on the training and validation data. In addition, the precision, sensitivity, specificity and F1-scores must be evaluated to confirm the model's reliability. By evaluating the confusion matrices, the F1-scores can be validated. In the case of Model 1, there were 12 instances of normal individuals being incorrectly diagnosed with bacterial pneumonia, two instances of COVID-19 misdiagnosis and 23 cases of projected viral pneumonia. As a result, there were numerous false positives, indicating a low level of accuracy.

The accuracy of the second model was significantly lower than that of Model 1 for both the training and validation data. The confusion matrix revealed that this method is not reliable for normal patient identification. There were 211 misclassified cases of bacterial pneumonia, 21 misclassified cases of COVID-19 and 36 misclassified cases of viral pneumonia. Due to the large amount of false positives, this model's recall was relatively low. The F1-score for this model was 0.49.

The third model had the highest training and validation accuracy, at 92.5% and 93.75%, respectively. Detection of COVID-19 is another strength of this approach. Thus, the model had a precision of 0.88 and a recall of 0.87. With a F1-score of 0.87, this model had the highest F1-score of any model examined.

Table 3. Summary of all models.

Models	**Accuracies (Train, Val)**	**Precision**	**Recall**	**F1-score**	**Confusion Matrix**
Model 1	Training accuracy: 0.8140 Validation accuracy: 0.9173	0.84	0.83	0.83	**B** 229, 3, 3, 97 **C** 0, 261, 0, 1 **N** 12, 2, 257, 23 **V** 28, 0, 9, 148
Model 2	Training accuracy: 0.8060 Validation accuracy: 0.8934	0.72	0.56	0.49	**B** 225, 0, 211, 138 **C** 10, 261, 21, 12 **N** 0, 0, 1, 0 **V** 34, 5, 36, 119
Model 3	Training accuracy: 0.9250 Validation accuracy: 0.9375	0.88	0.87	0.87	**B** 238, 3, 1, 83 **C** 0, 263, 0, 0 **N** 3, 0, 258, 9 **V** 28, 0, 10, 177

It was found that the model with the highest F1-score was the most accurate and trustworthy. Due to the fact that medical diagnosis relies significantly on false positives and false negatives, this is the case. A misdiagnosis can have severe repercussions, such as incorrect disease therapy or accelerated disease progression. Consequently, the third model, i.e., the fine-tuned MobileNetv2 model, is

considered to be the most reliable and effective model for this diagnosis in this experiment.

4. Discussions and conclusion, limitations and future research

4.1. Discussions

Since its first breakout at the end of 2019, COVID-19 has spread all across the world. Early identification of the illness is critical for preventing the spread of infectious diseases. An RT-PCR test for COVID-19 can offer a definitive diagnosis in patients with influenza-A viral pneumonia. There are some downsides to nucleic acid testing, such as a lack of availability, low detection rates and time delays. In the early stages of the disease, patients with COVID-19 may have excellent imaging results but little mucus and poor RT-PCR test results in nasopharyngeal swabs. These patients are not classified as suspected or confirmed cases. They are not separated or treated for the first time due to their possible role as a vector of infection. As a result, a machine learning-based technique is required.

The data for this study was obtained from the aforementioned web resources. Because many data sources were employed, the data had to be correctly integrated. The researcher used chest X-rays from healthy participants, as well as those with bacterial pneumonia, viral pneumonia and COVID-19 infection, to obtain the data. A 75:25 ratio was used to segregate the training data from the testing data. CNNs were used to build the models. Three models were made. The first model was a CNN trained from scratch on the dataset. The ResNet50 and MobileNetV2 networks were fine-tuned in the second batch of models. Pre-trained CNN models have also been used in previous works. A review of past research on the subject was also carried out. The performance of the three proposed models was evaluated by using a variety of criteria. Precision-recall values were evaluated, as well as the training and validation accuracy.

In terms of training and validation accuracy, as well as precision-recall values, MobileNetV2 came out on top. The model's accuracy on training data was 92.5%, and it was 93.75% on validation data. The precision, recall and F1-scores of this model were 0.88, 0.87 and 0.87, respectively.

Furthermore, this work demonstrates that fine-tuned transfer learning models do not always outperform models developed from scratch, as previously supposed. This was determined by employing the three models in this investigation. Model 1, which was built from the ground up, far outperformed the ResNet50 model. When compared to a fine-tuned version of MobileNetV2, MobileNetV2 outperformed the CNN model trained from scratch.

4.2. Conclusions

A novel computer-aided diagnosis method based on chest X-ray images and a fine-tuned MobileNetV2 model has been proposed here. The MobileNetV2 model was presented for accurate recognition of COVID-19 from chest X-ray images, and it can be used as a supplement to current advanced techniques such as RT-PCR to increase diagnostic certainty. As compared to previous models, the suggested model outperformed the more complicated and deeper CNN and ResNet50 models by 88%. The accuracy in this study was 88%, most likely due to the distinct form of COVID-19 that is associated with being asymptomatic. In addition to COVID-19 detection, the suggested method can detect both bacterial and viral pneumonia. Furthermore, more COVID-19 radiography datasets should be demonstrated for more reliability in terms of ability to construct robust and highly discriminative features to increase the accuracy of fine-tuned MobileNetV2 model tests [27].

4.3. Limitation

A lack of data contributed to several of the study's flaws. Neural networks, a type of machine learning system, perform optimally when provided with a huge quantity of data. Despite the numerous studies conducted, it is evident that machine learning has not yet had a significant impact in this area. Due to the paucity of COVID-19 data, machine learning methodologies sometimes require vast volumes of data for computer models to consume and collect knowledge. The creation, hosting and benchmarking of COVID-19-related datasets is critical because it can continue to drive disease-fighting discoveries. Structured criteria can be used to construct repositories for this purpose, allowing academics and scientists from all over the world to contribute and utilize them freely.

4.4. Future work

Further research may include the use of CT images in conjunction with X-ray images to provide clearer graphical information of the chest. This will assist models in learning more effectively and better grasping the various diseases. As the data show, distinguishing between bacterial and viral pneumonia is difficult for machine learning algorithms as well. Thus, incorporating more techniques that give the models a deeper context of the problem will assist in providing more accurate findings. Furthermore, many more kinds of pneumonia, such as CAP, can be included in the classification groups. Therefore, in the future, X-ray and CT images can be merged to provide a sharper picture of the chest. Researchers and clinicians would be able to understand the various diseases better as a result of this. These results may be relevant when suggesting exit strategies after a long-term quarantine. The results show that distinguishing between bacterial and viral pneumonia is difficult even for machine learning techniques. As a result, integrating more strategies to obtain models with a clearer context of the problem will yield better results. CAP, for example, can be included in the list of pneumonias that can be classified. Furthermore, it is feasible to go deeper into COVID-19's several stages, ranging from mild to severe. This is because those with mild COVID-19 symptoms require less attention and care than those with severe symptoms. Thus, using machine learning to estimate the severity of the illness is a significant breakthrough.

Acknowledgments

I would like to thank the reviewers for their constructive comments and reviews.

Conflict of interest

The author declares no conflict of interest.

References

1. A. A. Abdelhamid, E. Abdelhalim, M. A. Mohamed, F. Khalifa, Multi-classification of chest X-rays for COVID-19 diagnosis using deep learning algorithms, *Appl. Sci.*, **12** (2022), 2080. https://doi.org/10.3390/app12042080
2. W. S. McCulloch, W. Pitts, A logical calculus of the ideas immanent in nervous activity, *Bull. Math. Biophys.*, **5** (1943), 115–133.
3. Z. Li, F. Liu, W. Yang, S. Peng, J. Zhou, A survey of convolutional neural networks: Analysis,

applications and prospects, *IEEE Trans. Neural Netw. Learn Syst.,* **12** (2022), 6999–7019. https://doi.org/10.1109/TNNLS.2021.3084827

4. J. P. Cohen, L. Dao, K. Roth, P. Morrison, Y. Bengio, A. F. Abbasi, et al., Predicting COVID-19 pneumonia severity on chest X-ray with deep learning, *Cureus,* **12** (2020), e9448. https://doi.org/10.7759/cureus.9448
5. V. Ravi, H. Narasimhan, T. D. Pham, A cost-sensitive deep learning-based meta-classifier for pediatric pneumonia classification using chest X-rays, *Expert Syst.,* (2020), e12966. https://doi.org/10.1111/exsy.12966
6. I. Borlea, R. Precup, A. Borlea, D. Iercan, A unified form of fuzzy C-means and K-means algorithms and its partitional implementation, *Knowledge-Based Syst.,* **214** (2021), 106731. http://dx.doi.org/10.1016/j.knosys.2020.106731
7. D. Varshni, K. Thakral, L. Agarwal, R. Nijhawan, A.Mittal, Pneumonia detection using CNN based feature extraction, in *IEEE International Conference on Electrical, Computer and Communication Technologies (ICECCT),* (2019), 1–7.
8. M. Taresh, N. Zhu, T. A. A. Ali, Transfer learning to detect COVID-19 automatically from X-ray images, using convolutional neural networks, *Int. J. Biomed. Imaging,* (2021), 8828404. https://doi.org/10.1155/2021/8828404
9. S. R. Velu, V. Ravi, K. Tabianan, Data mining in predicting liver patients using classification model, *Health Technol. (Berl),* **12** (2022),1211–1235. https://doi.org/10.1007/s12553-022-00713-3
10. M. H. Alsharif, Y. H. Alsharif, K. Yahya, O. A. Alomari, M. A. Albreem, A. Jahid, Deep learning applications to combat the dissemination of COVID-19 disease: A review, *Eur. Rev. Med. Pharmacol. Sci*., **24** (2020), 11455–11460. https://doi.org/10.26355/eurrev_202011_23640
11. S. Sharma, Drawing insights from COVID-19-infected patients using CT scan images and machine learning techniques: A study on 200 patients, *Environ. Sci. Pollut. Res.*, **27** (2020), 37155–37163. https://doi.org/10.1007/s11356-020-10133-3
12. A. Narin, C. Kaya, Z. Pamuk, Automatic detection of coronavirus disease (COVID-19) using X-ray images and deep convolutional neural networks, *Pattern Anal, Appl.*, **24** (2021), 1207–1220. https://doi.org/10.1007/s10044-021-00984-y
13. H. Panwar, P. K. Gupta, M. K. Siddiqui, R. Morales-Menendez, V. Singh, Application of deep learning for fast detection of COVID-19 in X-Rays using nCOVnet, *Chaos Solitons Fract.,* **138** (2020), 109944. https://doi.org/10.1016/j.chaos.2020.109944
14. M. Singh, S. Bansal, S. Ahuja, R. K. Dubey, Panigrahi, B. K. Dey, Transfer learning–based ensemble support vector machine model for automated COVID-19 detection using lung computerized tomography scan data, *Med. Biol. Eng. Comput*., **59** (2021), 825–839. https://doi.org/10.1007/s11517-020-02299-2
15. A. M. Alqudah, S. Qazan, A. Alqudah, Automated systems for detection of COVID-19 using chest X-ray images and lightweight convolutional neural networks, *Emerg. Radiol.,* **4** (2020). https://doi.org/10.1007/s13246-020-00865-4
16. I. D. Apostolopoulos, T. A. Mpesiana, COVID-19: Automatic detection from X-ray images utilizing transfer learning with convolutional neural networks, *Phys. Eng. Sci. Med.,* **43** (2020), 635–640. https://doi.org/10.1016/j.eng.2020.04.010
17. X. Xu, X. Jiang, C. Ma, P. Du, X. Li, S. Lv, et al., deep learning system to screen novel A Coronavirus Disease 2019 pneumonia, *Engineering,* **6** (2020), 1122–1129. https://doi.org/10.1016/j.eng.2020.04.010

18. E. Hussain, M. Hasan, M. A. Rahman, I. Lee, T. Tamanna, M. Z. Parvez, CoroDet: A deep learning based classification for COVID-19 detection using chest X-ray images, *Chaos Solitons Fract.*, **142** (2021), 110495. https://doi.org/10.1016/j.chaos.2020.110495
19. S. Wang, B. Kang, J. Ma, X. Zeng, M. Xiao, J. Guo, et al., A deep learning algorithm using CT images to screen for Corona Virus Disease (COVID-19), *Eur Radiol.*, **31** (2021), 6096–6104. https://doi.org/10.1007/s00330-021-07715-1
20. L. L, L. Qin, Z.Xu, Y. Yin, X. Wang, B. Kong, et al., Artificial intelligence distinguishes COVID-19 from community acquired pneumonia on chest CT, *Radiology*, **296** (2020). https://doi.org/10.1148/radiol.2020200905
21. A. N. J Raj, H. Zhu, A. Khan, Z. Zhuang, Z. Yang, V. G. V. Mahesh, et al., ADID-UNET—a segmentation model for COVID-19 infection from lung CT scans, *PeerJ Comput. Sci.*, **7** (2021), e349. https://doi.org/10.7717/PEERJ-CS.349
22. H. Khalid, M. Hussain, M. A. Al Ghamdi, T. Khalid, K. Khalid, M. A. Khan, et al., A comparative systematic literature review on knee bone reports from MRI, X-rays and CT scans using deep learning and machine learning methodologies, *Diagnostics*, **10** (2020), 518. https://doi.org/10.3390/diagnostics10080518
23. G. Puneet, Pneumonia detection using convolutional neural networks, *Int. J. Sci. Technol. Res.*, **7** (2021), 77–80. https://doi.org/10.46501/ijmtst070117
24. X. Ding, Y. Guo, G. Ding, J. Han, Acnet: Strengthening the kernel skeletons for powerful CNN via asymmetric convolution blocks, in *IEEE/CVF international conference on computer vision (ICCV)*, (2019), pp. 1911–1920. http://dx.doi.org/10.1109/ICCV.2019.00200
25. S. Kostadinov, What is deep transfer learning and why is it becoming so popular? *Towards Data Science*, (2019).
26. M. Lascu, Deep learning in classification of Covid-19 coronavirus, pneumonia and healthy lungs on CXR and CT images, *J. Med. Biol. Eng.*, **41** (2021), 514–522. http://dx.doi.org/10.1007/s40846-021-00630-2
27. X. Ma, B. Zheng, Y. Zhu, F. Yu, R. Zhang, B. Chen, Covid-19 lesion discrimination and localization network based on multi-receptive field attention module on CT images, *Optik*, **241** (2021), 167100. http://dx.doi.org/10.1016/j.ijleo.2021.167100
28. R. Kundu, R. Das, Z. W. Geem, G. T. Han, R. Sarkar, Pneumonia detection in chest X-ray images using an ensemble of deep learning models, *PLoS One*, **16** (2021), e0256630. https://doi.org/10.1371/journal.pone.0256630

AIMS Press